Laser Light Scattering Study of the Formation and Structure of Poly(*N*-isopropylacrylamide-*co*-acrylic acid) Nanoparticles

Xingping Qiu, Chi Man Simon Kwan, and Chi Wu*

Department of Chemistry, The Chinese University of Hong Kong, Shatin, N.T., Hong Kong

Received April 9, 1997; Revised Manuscript Received June 25, 1997[⊗]

ABSTRACT: Poly(*N*-isopropylacrylamide-*co*-acrylic acid) (PNIPAM-*co*-AA) ionomer chains can form stable nanoparticles in water at temperatures higher than their lower critical solution-temperature. A combination of the weight average molar mass (M_w) from the absolute average scattering intensity and the hydrodynamic radius distribution ($f(R_h)$) from the line width distribution $G(\Gamma)$ was used to study the influence of the AA content and molar mass of the ionomer chains on the formation and structure of these novel surfactant-free nanoparticles. Our results reveal (1) particle size decreases as the AA content increases; (2) the particle formation is not only thermodynamically controlled but also dependent on the formation temperature, the polymer concentration, and the molar mass of the ionomer chains, because it involves simultaneously the process of the intrachain collapse and interchain aggregation; and (3) the hydrodynamic density ($\langle\rho\rangle$) of the particle slightly increases as the formation temperature increases but remains to be a constant when the ionomer concentration varies. We also found that the weight average particle mass ($M_{w,particle}$) can be scaled with the ionomer concentration (C) as $M_{w,particle} \propto C^{2/3}$, revealing that the aggregation is a diffusion-controlled process.

Introduction

Poly(*N*-isopropylacrylamide) (PNIPAM) is a well-known thermal sensitive polymer.[1,2] It is soluble in water at room temperature but undergoes a phase separation at temperatures higher than its lower critical solution temperature (LCST, ∼32 °C). It is this unusual and convenient phase transition temperature and its related solution properties that have attracted much theoretical and technological interests.[3−10] It is commonly believed that this convenient LCST is the results of a delicate balance between the hydrophobic and hydrophilic interactions. At higher temperatures, the term related to the negative entropy change leads a positive free energy change, i.e., $\Delta G = \Delta H - T\Delta S > 0$, so that individual PNIPAM chains collapse and aggregate in water.[2]

Recently, it has been found that randomly carboxylated polystyrene ionomer chains can form stable colloidal nanoparticles in water if a dilute solution of an ionomer in tetrahydrofuran (THF) is added dropwise into an excessive amount of water. The average surface area occupied per ionic group was found to be a fundamental parameter to determine the final particle size in the dispersion.[11] On the other hand, Deng and Pelton[12] found that (1) introducing a very small amount of ionic groups into PNIPAM could lead to stable PNIPAM aggregates at temperatures higher than the LCST and (2) the final size of the aggregates varied in the range of 50−250 nm, depending on the ionic content, temperature, pH, and the salt concentration. We realize that their results have provided a convenient way to study the formation and structure of surfactant-free colloidal nanoparticles stabilized by ionic groups on the particle surface. Therefore, a set of poly(*N*-isopropylacrylamide-*co*-acrylic acid) ionomers with desired ionic contents and molar masses were prepared. Laser light scattering (LLS) study of the formation and structure of the nanoparticles made of these PNIPAM copolymers are reported as follows.

[⊗] Abstract published in *Advance ACS Abstracts,* August 15, 1997.

Table 1. Molecular Parameters of Poly(*N*-isopropylacrylamide-*co*-acrylic acid) Ionomers

samples	M_w (g/mol) in H_2O	M_w (g/mol) in THF	AA (mol %)	$\langle R_g\rangle$ (nm)	CPT (°C)
PNIPAM-0.8AA	4.6×10^6	4.7×10^6	0.8	121.0	33
PNIPAM-1.1AA	7.6×10^4	7.4×10^4	1.1	11.4	37
PNIPAM-2.0AA	9.1×10^4	8.9×10^4	2.0	13.7	39
PNIPAM-4.0AA	8.2×10^4	6.8×10^4	4.0	10.8	42
PNIPAM-6.2AA	8.6×10^4	8.3×10^4	6.2	13.3	

Experimental Section

Laser Light Scattering. The experimental setup and basic theory were detailed before.[13,14] In static LLS, the angular and concentration dependence of the average excess scattering intensity leads to the weight average molar mass (M_w) and the average radius of gyration $\langle R_g\rangle$. In dynamic LLS, the intensity−intensity time correlation function was measured, which leads to the hydrodynamic radius distribution ($f(R_h)$). All the dynamic light-scattering experiments were made at $\theta = 15°$ except otherwise stated. The specific refractive index increments (dn/dC) of the polymer in water are 0.167 mL/g at 25 °C and 0.172 mL/g at 45 °C.[13] Polymer solutions were clarified using 0.5 or 0.1 μm Millipore filters, depending on the size of the particle.

Ionomer Synthesis. The copolymers of *N*-isopropylacrylamide (NIPAM) and acrylic acid (AA) were prepared by free-radical polymerization at 60 °C using azobis(isobutyronitrile) (AIBN) as the initiator and a benzene/ethanol mixture as the reaction medium. Details of the synthesis has already been reported.[15] NIPAM monomer (courtesy of Kohjin Co., Japan) was purified by recrystallization in a benzene/*n*-hexane mixture. The AA monomer was distilled under reduced pressure at 40 °C to remove the inhibitant. AIBN was recrystallized in methanol. All the solvents used were analytical grade and freshly distilled. Each ionomer product was purified through three cycles of the acetone-to-hexane reprecipitation. Here, the acid form of poly(NIPAM-*co*-AA) is denoted as PNIPAM-*m*AA, while the ionomers neutralized with different bases are correspondingly labeled as PNIPAM-*m*MAA, where *m* represents the average mole content of AA in each ionomer chain and *M* represents the cation of the base used to neutralize the ionomer. The molecular parameters of individual ionomer chains, such as M_w, $\langle R_g\rangle$, and the AA content are summarized in Table 1.

S0024-9297(97)00484-1 CCC: $14.00

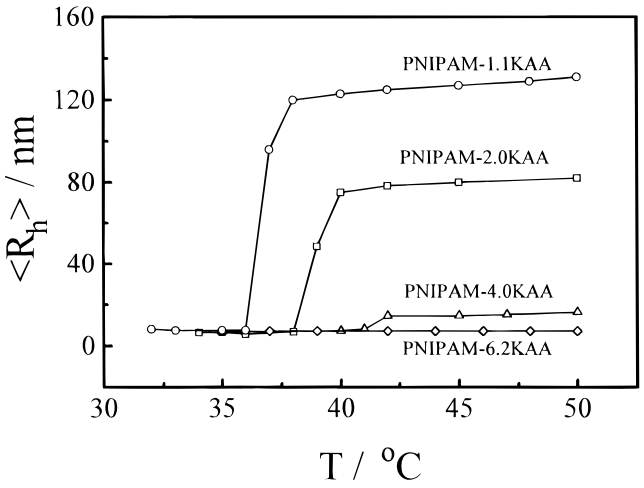

Figure 1. Temperature dependence of the average hydrodynamic radius $\langle R_h \rangle$ of four low molar mass PNIPAM-*m*KAA ionomers in water, where $C = 5.0 \times 10^{-4}$ g/mL.

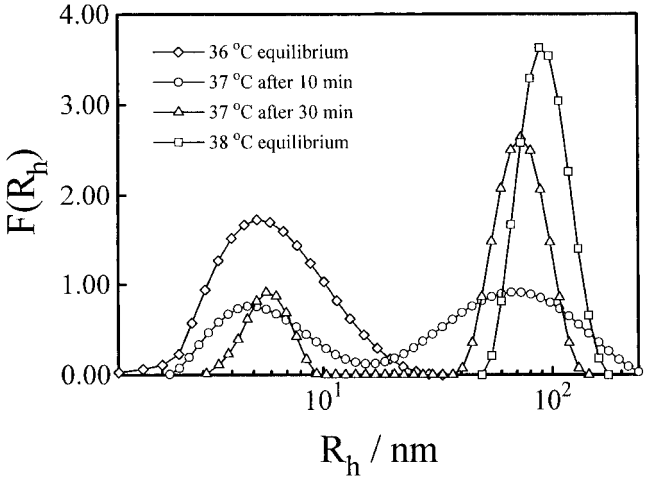

Figure 2. Temperature and time dependence of the hydrodynamic radius distribution ($f(R_h)$) of PNIPAM-1.1KAA in water, where $C = 5 \times 10^{-4}$ g/mL.

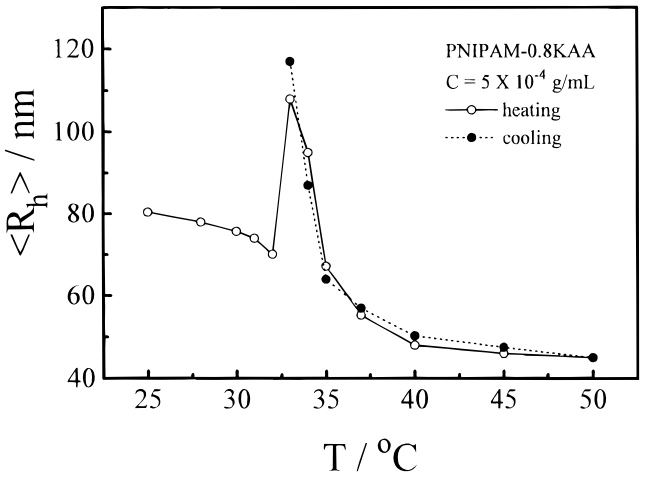

Figure 3. Temperature dependence of the average hydrodynamic radius of a high molar mass ionomer PNIPAM-0.8KAA in water, $C = 5 \times 10^{-4}$ g/mL.

Results and Discussion

Figure 1 shows the temperature dependence of the average hydrodynamic radius $\langle R_h \rangle$ of four PNIPAM-*m*KAA ionomers with different ionic contents, but a similar average molar mass ($M_w \sim 8 \times 10^4$ g/mol), where $C = 5.0 \times 10^{-4}$ g/mL. Except for PNIPAM-6.2KAA, a distinct increase of $\langle R_h \rangle$ for each ionomer was observed at a certain higher temperature. It is believed that even for PNIPAM-6.2KAA there should also exist a sharp increase of $\langle R_h \rangle$ at a higher temperature outside the temperature range studied. This sharp increase in $\langle R_h \rangle$, accompanied with a sharp increase of the scattered light intensity (not shown), clearly indicates the aggregation of individual ionomer chains in solutions.[16] Note that this turning point is commonly defined as the cloud point temperature (CPT).[12] Figure 1 shows that when temperature is lower than the CPT, the solution contains only individual ionomer chains since $\langle R_h \rangle$ (~7−8 nm) is very small, and at the CPT, individual ionomer chains start to aggregate to form large aggregates (particles). It was interesting to find that $\langle R_h \rangle$ is nearly independent of temperature in the high-temperature range, showing that, after the formation, the particles are quite stable against the temperature change. The final particle size increases as the ionic content decreases, very similar to the aggregation of the carboxylized polystyrene ionomers in water.[11] It is also reasonable to see that the CPT increases as the amount of the hydrophilic AA groups increases, which has also been observed in other ionomer systems.[3,8,17] It should be pointed out that the type of counter ions has no obvious effect on the CPT, indicating that the aggregation is mainly controlled by the hydrophobic interaction between the NIPAM segments.

Figure 2 shows the temperature dependence of the hydrodynamic radius distribution of PNIPAM-1.1KAA in water, where $C = 5 \times 10^{-4}$ g/mL. At 36 °C, which is slightly lower than the CPT, there exists only one peak located at ~7 nm, corresponding to individual ionomer chains. After the ionomer is heated to 37 °C, another peak appears at ~80 nm, reflecting the aggregation of individual ionomer chains. It is understandable that the area of the first peak (individual chains) decreases and the second peak (the aggregates) increases as time increases, (i.e., the aggregation proceeds). The aggregation equilibrium was reached within ~1 h at 37 °C. Further increase of temperature leads to a shift of the aggregation equilibrium. At 38 °C, the first peak completely disappears, indicating the aggregation of all the ionomer chains. The equilibrium is possibly determined by the two following factors: (1) the inhomogeneity of the ionic content, i.e., the ionomer chains have different ionic contents around the average values, so that at 37 °C the ionomer chains with a relatively lower ionic content collapse and aggregate first and those with a higher ionic content still remain to be individual in the solution and (2) the hydrophobic interaction, i.e., even if the ionic content was uniform, the hydrophobic interaction at a lower temperature is weaker, so that there exists an equilibrium between individual chains and aggregates. It is worth noting that at 37 °C the position of the second peak remains unchanged in the aggregation process, indicating that the average size of the aggregates is a constant at a given temperature. The plateau of $\langle R_h \rangle$ shown in Figure 1 also indicates a nearly constant particle size for a given condition. The question is what has determined the final size of the ionomer aggregates. We will come back to this point after examining the aggregation of much longer ionomer chains.

Figure 3 shows the temperature dependence of the average hydrodynamic radius of the high molar mass ionomer (PNIPAM-0.8KAA) in water, where $C = 5 \times 10^{-4}$ g/mL. The phase transition temperature is also

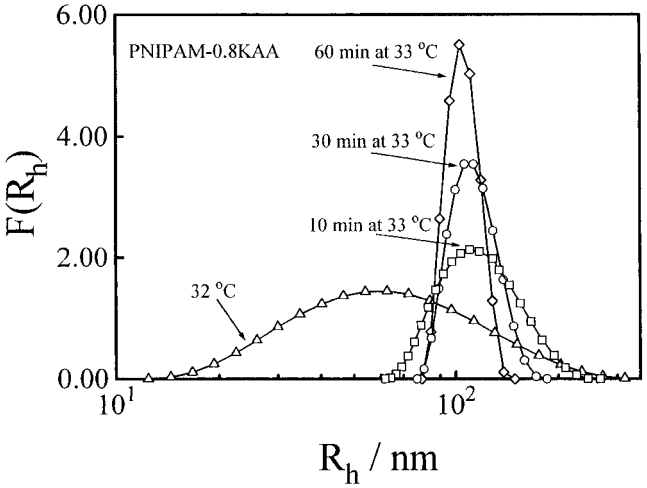

Figure 4. Temperature and time dependence of the hydrodynamic radius distribution $f(R_h)$ of PNIPAM-0.8KAA in water, where $C = 5 \times 10^{-4}$ g/mL.

evidenced by the abrupt change of $\langle R_h \rangle$. In contrary to the case of the low molar mass PNIPAM-KAA ionomers shown in Figure 1, $\langle R_h \rangle$ decreases as temperature increases when temperature is lower than the phase transition temperature. Moreover, $\langle R_h \rangle$ decreases after reaching a maximum and finally comes down to a low plateau. We think that this difference actually reflects the competition between the intra- and interchain interactions. For short chains, the intrachain collapse has less effect on the overall chain dimension and is faster than the interchain aggregation; while for longer chains, before reaching the phase transition temperature, water gradually becomes a poor solvent, so that individual ionomer chains undergo an intrachain collapse;[18] and at the phase transition temperature, the intrachain collapse and the interchain aggregation are expected to occur simultaneously because the overlap concentration for longer chains is lower. In the aggregation process, the average number of the ionic groups in each particle is proportional to the particle mass ($M_{particle}$), while the surface area of the particle is only proportional to $M_{particle}^{2/3}$ if the particle has a uniform chain density. Therefore, the surface area per ionic group (S_{ionic}) is proportional to $M_{particle}^{-1/3}$. As $M_{particle}$ increases, S_{ionic} decreases. At the same time, the intrachain collapse also decreases S_{ionic}. When S_{ionic} decreases to a certain value, the aggregation stops because the ionic repulsion between different particles stabilizes the aggregates. However, the intrachain collapse continues. This is why $\langle R_h \rangle$ first increases and then decreases.

Figure 4 shows the annealing time dependence of the hydrodynamic radius distribution $f(R_h)$ of the high molar mass ionomer chains in water after the solution is brought from 32 to 33 °C, where $C = 5 \times 10^{-4}$ g/mL. The increase of temperature to 33 °C shifts the peak position to a higher R_h value, clearly indicating the aggregation of individual ionomer chains. The shift of the peak position to a lower R_h value as the annealing time increases can be attributed to the intrachain collapse. In comparison with $F(R_h)$ at 32 °C, $F(R_h)s$ at 33 °C are narrower. Because the aggregation of individual chains with different molar masses is an averaging process, the aggregates are normally narrower than individual chains.[19,20]

Figure 5 shows a schematic of two different nanoparticle formation processes on the basis of Figures 1−4,

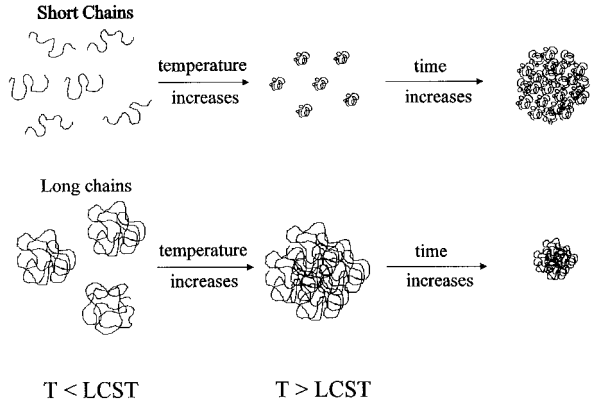

Figure 5. Schematic of two different particle formation processes respectively for short and long ionomer chains.

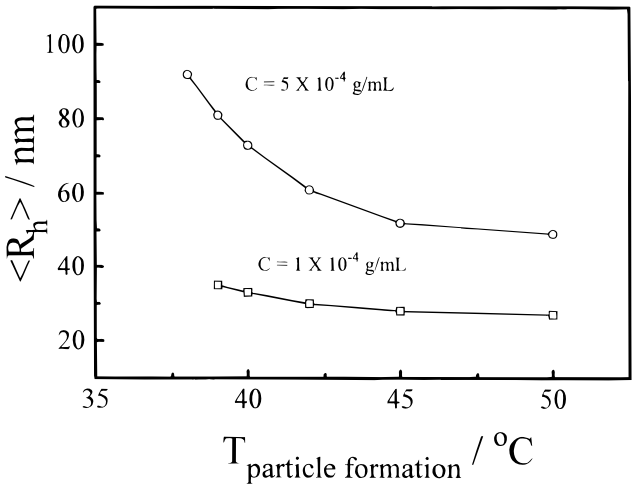

Figure 6. Formation temperature dependence of the average hydrodynamic radius $\langle R_h \rangle$ of PNIPAM-1.1KAA particles.

namely, for low molar mass chains, most of the individual ionomer chains collapse before their aggregation, while for high molar mass chains, it seems that the interchain aggregation is precedes the intrachain collapses. It is worth to note a previous report[21,22] that the "coil-to-globule" transition of the PNIPAM homopolymer in dilute aqueous solution is not an "all-or-none" process, namely, the collapse of the PNIPAM chain involves a cooperative collapse of a series of independent chain segments with a molar mass in the order of $\sim 6 \times 10^4$ g/mol. If it were true, on average, our low molar mass ionomer chains have only one such segment so that the intrachain collapses prior to the interchain aggregation because it involves no cooperative chain movement, but for high molar mass ionomer chains, a mixture of the interchain aggregation and the intrachain collapse is expected. Our results indirectly support that the coil-to-globule transition of a polymer chain is not an all-or-none process.

It is important to state that the variation of $\langle R_h \rangle$ with temperature is reversible in the temperature range studied as shown in Figure 3 by the dashed line, but the time required to reach the equilibrium state is quite different between the heating and cooling processes. For example, after the solution is heated from 32 to 33 °C, the aggregation equilibrium was reached within ~1 h, while in the reverse process of cooling down from 33 to 32 °C, the dissociation of the aggregates took a much longer time (~5 h), which can be attributed to the chain entanglements in the aggregates. As mentioned before, the size of the colloidal particles formed through the

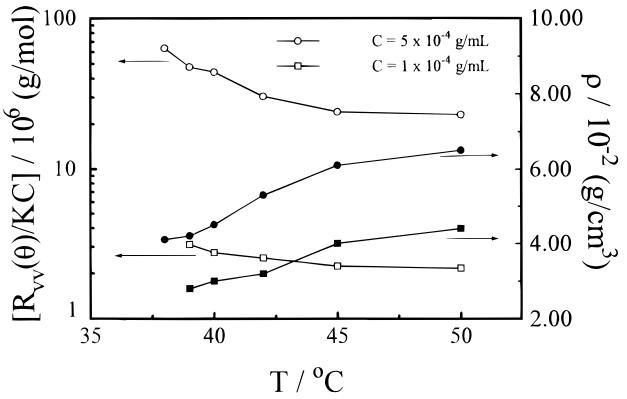

Figure 7. Formation temperature dependence of the excess scattering intensity ($R_{vv}(\theta)/KC$) and the average chain density ($\langle\rho\rangle$) of the PNIPAM-1.1KAA particles, where $\langle\rho\rangle = M_{w,particle}/{}^4/_3\pi N_A\langle R_h\rangle^3$.

aggregation of the PNIPAM-KAA ionomer chains at higher temperatures are influenced by the solution temperature, ionic content, and polymer concentration, or in other words, the colloidal particles were in a metastable state. This metastable nature can be better viewed from the formation temperature dependence of the particle size for a given ionomer solution.

Figure 6 shows the average hydrodynamic radii of the PNIPAM-1.1KAA particles formed at different temperatures, where the solution was brought everytime up to the formation temperature by one jump from 25 °C. It should be stated that, after the formation of the particles at each temperature, a further increase in temperature has nearly no effect on $\langle R_h\rangle$ because the formation temperatures are already higher than the LCST. Figure 6 shows (1) the higher the formation temperature, the smaller the particles will be and (2) the higher the polymer concentration, the larger the particles will be. If considering the competition between the intrachain collapse and the interchain aggregation, it is not difficult for us to understand Figure 6. When the temperature was quickly increased from 25 °C to a temperature higher than the LCST, individual ionomer chains start to shrink (the coil-to-globule transition). In the shrinking process, the ionic groups have a tendency to stay at the surface of the collapsed chains, and the surface area per ionic group decreases as the shrinking proceeds so that the collapsed ionomer chains can be stabilized by the ionic groups on the surface. The higher the formation temperature, the faster the shrinking of the ionomer chains will be so that individual ionomer chains have less of a chance to aggregate with each other to form larger particles. For the same reason, in a lower concentration, individual ionomer chains have less chances to undergo the interchain aggregation so that the particles formed are smaller.

Figure 7 shows the formation temperature dependence of the excess scattering intensity of the PNIPAM-1.1KAA particles. It is known that $R_{vv}(q)/KC$ is proportional to the weight average molar mass ($M_{w,particle}$) of the particles. The decrease of $R_{vv}(q)/KC$ clearly indicates that on average the number of the ionomer chains in each particle decreases as the formation temperature increases, which supports our previous explanation of Figure 7. A combination of $M_{w,particle}$ and $\langle R_h\rangle$ at each temperature leads to the average chain density ($\langle\rho\rangle$) of the particles by using $\langle\rho\rangle = M_{w,particle}/[(4/3)\pi N_A\langle R_h\rangle^3]$, which are also shown in Figure 7. The slight increase of $\langle\rho\rangle$ reflects that the decrease of $\langle R_h\rangle$ is faster than the decrease of $M_{w,particle}$, or in other words, the extent of the chain collapse increases as the formation temperature increases.

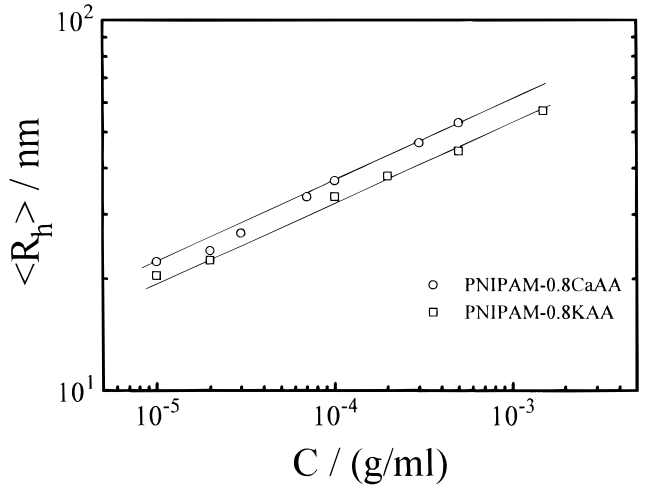

Figure 8. Concentration dependence of $\langle R_h\rangle$ of the PNIPAM-0.8KAA and PNIPAM-1.1CaAA particles formed at 45 °C.

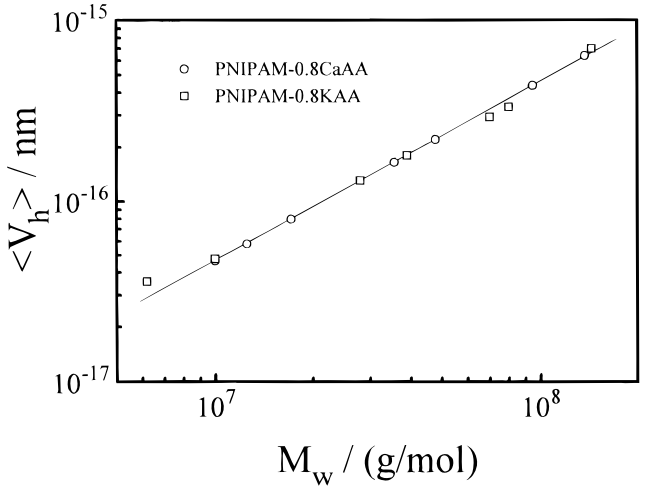

Figure 9. Plots of the weight average molar mass of the particles ($M_{w,particle}$) *versus* the average hydrodynamic volume ($\langle V_h\rangle$) at 45 °C, where $\langle V_h\rangle$ is defined as ${}^4/_3\pi\langle R_h\rangle^3$ and the line represents a least squares fitting of $M_{w,particle} = 2.06 \times 10^{23}\text{-}\langle V_h\rangle$.

Figure 8 respectively shows the concentration dependence of $\langle R_h\rangle$ of the PNIPAM-0.8KAA and PNIPAM-0.8CaAA aggregates formed at 45 °C. PNIPAM-0.8CaAA particles are slightly larger than the corresponding PNIPAM-0.8KAA particles. It is interesting to see that $\log(\langle R_h\rangle)$ is proportional to $\log(C)$ in the concentration range $(5 \times 10^{-4})-(1 \times 10^{-5})$ g/mL. The lines represent the least squares fittings of $\langle R_h\rangle = 2.51 \times 10^2 C^{0.22}$ and $\langle R_h\rangle = 2.61 \times 10^2 C^{0.22}$ for NIPAM-0.8KAA and NIPAM-0.8CaAA, respectively. The same exponent indicates that the type of the counter ion has no effect on the particle formation mechanism. As we have discussed before, it is understandable that the particle size increases as the polymer concentration increases because in a higher concentration the ionomer chains have more chance to undergo the interchain aggregation before they are stabilized by the ionic groups on the particle surface.

Figure 9 shows that the weight average particle mass ($M_{w,particle}$) from static LLS is linearly proportional to the average hydrodynamic volume ($\langle V_h\rangle$) of the particles, which convincingly demonstrates that the average chain density ($\langle\rho\rangle$) of the particles is a constant and the

particles are uniform in the chain density. $\langle\rho\rangle$ is directly related to the slope of the line because $M_{w,particle} = \langle\rho\rangle N_A\langle V_h\rangle$, where N_A is the Avogadro constant. A least squares fitting leads to $M_{w,particle} = 2.06 \times 10^{23}\langle V_h\rangle$ so that $\langle\rho\rangle = 0.342$ g/cm^3. Obviously, the long chain ionomer aggregates have a much higher $\langle\rho\rangle$ than the short chain ionomer aggregates shown in Figure 7, which is understandable on the basis of Figure 5. For short chains, the intrachain collapse followed by the aggregation of the collapsed chains cannot reach the density of the interchain aggregates. It should be pointed out that, even for the long chain ionomer aggregates, the value of $\langle\rho\rangle = 0.342$ g/cm^3 is still much lower than a normal polymer density ($\sim$1 g/cm^3) in bulk, indicating that the particles contain $\sim$60$-$70% water in its hydrodynamic volume. Finally, a combination of Figures 8 and 9 leads to $M_{w,particle} \propto C^{2/3}$.

Conclusions

Poly(*N*-isopropylacrylamide-*co*-acrylic acid) (PNIPAM-*co*-AA) ionomers can form stable nanoparticles in water through the intrachain collapse and interchain aggregation at temperatures higher than the low critical solution temperature (LCST). For a given chain length, the LCST increases as the AA content increases. The particle size can be well controlled by the molar mass of the ionomer chain, the ionic content, the ionomer concentration, and the particle formation temperature. If other conditions are fixed, the increase of the molar mass or the ionomer concentration leads to larger particles, while the increase of the ionic content or the particle formation temperature leads to smaller particles. In other words, promoting the interchain aggregation or suppressing the intrachain collapse leads to larger particles. For a given ionomer, the particle density slightly increases as the particle formation temperature increases, while for a given formation temperature, the particle density is independent of the polymer concentration. Our results show that the weight average molar mass of the particles ($M_{w,particle}$) can be scaled with the ionomer concentration (C) as $M_{w,particle} \propto C^{2/3}$. It is known that the average interchain distance (L) is proportional to $1/C^{1/3}$ and $L^2 = 2Dt$ so that $M_{w,particle} \propto C^{2/3} \propto 1/2Dt$, indicating that the aggregation is a diffusion-controlled process.

Acknowledgment. The financial support of the Research Grants Council of Hong Kong Government Earmarked Grant 1995/1996 (CUHK 305/96P, A/C No. 2160063) is gratefully acknowledged.

References and Notes

(1) Heskins, M.; Guillet, J. E. *J. Macromol. Sci. Chem.* **1969**, *2*, 1441.
(2) Schild, H. G. *Prog. Polym. Sci.* **1992**, *7*, 163 and references therein.
(3) Guillet, J. E.; Heskins, M.; Murray, D. G. U.S. Patent 4,536,294, 1985.
(4) Dong, L. C.; Yan, Q.; Hoffman, A. S. *J. Controlled Release* **1992**, *19*, 171.
(5) Hayashi, H.; Kono, K.; Takagishi, T. *Biochim. Biophys. Acta* **1996**, *1280*, 127.
(6) Wu, C.; Zhou, S. *Macromolecules* **1995**, *28*, 8381.
(7) Deng, Y.; Xiao, H.; Pelton, R. *J. Colloid Interface Sci.* **1996**, *179*, 188.
(8) Hirotsu, S.; Hirokawa, Y.; Tanaka, T. *J. Chem. Phys.* **1987**, *87*, 1392.
(9) Beltran, S.; Baker, J. P.; Hooper, H. H.; Blanch, H. W.; Prausnitz, J. M. *Macromolecules* **1991**, *24*, 549.
(10) Ringsdorf, H.; Sackmann, E.; Simon, J.; Winnik, F. M. *Biochim. Biophys. Acta* **1993**, *1153*, 335.
(11) Li, M.; Jiang, M.; Wu, C. *Macromolecules* **1997**, *30*, 2201.
(12) Deng, Y.; Pelton, R. *Macromolecules* **1995**, *28*, 4617.
(13) Zhou, S. Q.; Fan, S. Y.; Au-yeung, S. T. F.; Wu, C. *Polymer* **1995**, *36*, 1341.
(14) Wu, C.; Zhou, S. *Macromolecules* **1996**, *29*, 1574.
(15) Qiu, X.; Wu, C. *Polymer* **1997**, accepted for publication.
(16) Zhou, Z.; Chu, B.; Peiffer, D. G. *Macromolecules* **1991**, *24*, 5811.
(17) Tiktopulo, E. I.; Bychkova, V. E.; Ricka, J.; Ptitsyn, O. B. *Macromolecules* **1994**, *27*, 2879.
(18) Winnik, F. M. *Polymer* **1990**, *31*, 2125.
(19) Zhang, Y.; Wu, C.; Fang, Q.; Zhang, Y. *Macromolecules* **1996**, *29*, 2494.
(20) Wu, C.; Wu, P.; Ma, X. *J. Polym. Sci., Polym. Phys.* **1996**, *34*, 211.
(21) Meewes, M.; Ricka, J.; Silva, M. de; Nyffenegger, R.; Binkert, Th. *Macromolecules* **1991**, *24*, 5811.
(22) Wu, C.; Zhou, S. *Phys. Rev. Lett.* **1996**, *77* (14), 3053.

MA970484S